

Comparison of Cortical and Cutaneous Vascular Hemodynamic Changes in Hypoxia by Using *in Vivo* Skull and Skin Optical Clearing Techniques

Wei Feng , Chao Zhang, and Dan Zhu

Abstract—Hypoxia occurs in various pathophysiological conditions. Especially, brain can be seriously affected by the oxygen deficiency. However, challenges exist in optically monitoring cerebral hemodynamics with high resolution. As an easily-detected vessel bed, peripheral skin is a potential target for predicting cerebrovascular hemodynamic changes. However, the similarities and differences between cerebral and cutaneous hemodynamics during hypoxia are still unclear. One of the main reasons is that optical imaging techniques are fundamentally depth/resolution-limited due to high scattering properties of turbid tissue. Fortunately, *in vivo* tissue optical clearing techniques can efficiently overcome these problems, and avoid the side-effects of surgical windows. In this work, we simultaneously monitor the changes in cortical and cutaneous microvascular blood oxygen and blood flow under the assistance of *in vivo* skull and skin optical clearing techniques, and quantitatively compared the differences between cerebral and cutaneous arteriovenous functional responses to the hypoxic stimulus. The results indicated that the variation tendency of blood oxygen response might be more similar, and cutaneous vascular blood oxygen response has the potential to serve as an accessible indicator for revealing cerebrovascular dysfunction. Moreover, it provides a feasible approach to realize visualization of *in vivo* monitoring cerebral and cutaneous microvascular reactivity with minimal invasiveness.

Index Terms—Hyperspectral imaging, hypoxia, laser speckle contrast imaging, skin optical clearing, skull optical clearing.

I. INTRODUCTION

TISSUE hypoxia plays an important role in the pathophysiology of various human disorders, e.g., ischemic cardiovascular disease, stroke, chronic lung disease, acute skin wounds

Manuscript received October 15, 2020; revised January 22, 2021; accepted February 22, 2021. Date of publication February 26, 2021; date of current version March 30, 2021. This work was supported in part by the National Natural Science Foundation of China (NSFC) under Grants 61860206009, 81870934, and 82001266, and in part by Guangdong Basic and Applied Basic Research Foundation under Grants 2019A1515110699, 2019A1515110803, 2021A1515011783, and 2021A1515011443. (Corresponding authors: Chao Zhang; Dan Zhu.)

Wei Feng and Chao Zhang are with the Zhanjiang Institute of Clinical Medicine, Central People's Hospital of Zhanjiang, Zhanjiang 524045, China (e-mail: fenywei@qq.com; 546329296@qq.com).

Dan Zhu is with the Britton Chance Center for Biomedical Photonics, Wuhan National Laboratory for Optoelectronics, Huazhong University of Science and Technology, Wuhan 430074, China, and also with the MoE Key Laboratory for Biomedical Photonics, School of Engineering Sciences, Huazhong University of Science and Technology, Wuhan 430074, China (e-mail: dawnzh@mail.hust.edu.cn).

Color versions of one or more figures in this article are available at <https://doi.org/10.1109/JSTQE.2021.3062595>.

Digital Object Identifier 10.1109/JSTQE.2021.3062595

and cancer [1]–[4]. As one of the most important organs, the brain needs continuous and adequate supply of oxygen to maintain its structural and functional integrity, and even moderate reduction in oxygen delivery can cause serious brain dysfunction [5], [6]. Also, the hypoxia has an effect on other tissues and organs including peripheral skin [7]. There have been some researches investigate the changes in blood flow or blood oxygen of brain and skin by using various techniques, i.e., Duong *et al.* employed MRI to monitor the cerebral blood flow velocity changes induced by hypoxia [8]; Palmer *et al.* used spectral imaging to investigate the cutaneous blood oxygen changes around the tumor [9]. However, the imaging resolutions of these approaches have been greatly limited.

Nowadays, optical imaging techniques have received more and more attentions in studying microvascular functions thanks to the advantage in the high resolution, such as optical coherence tomography (OCT), photoacoustic tomography, multiphoton microscopy, laser speckle contrast imaging (LSCI) and hyperspectral imaging technique (HSI). However, the high scattering properties of skin and skull seriously limit the imaging depth and resolution. Fortunately, the optical clearing imaging windows established by *in vivo* optical clearing techniques provide the powerful tools to effectively improve both imaging depth and contrast in various optical imaging modalities without applying general imaging windows based on the complex surgeries. The recently-developed skin optical clearing technique can greatly enhance the imaging qualities in confocal microscopy [10], photoacoustic tomography [11], [12], OCT [13]–[15], LSCI [16] and HSI [17], allowing to observe the immunocyte movement [10], as well as the structural and functional changes in cutaneous vessels [18], [19]. In addition, the skull optical clearing technique permits us to monitor the neuronal synapse growth in young mice [20], and the cerebrovascular dynamics under physiopathological conditions [21]–[23].

Compared with the brain, peripheral skin is a more accessible and generalized vascular bed for clinical diagnosis. Some studies have identified that the peripheral skin has a great potential to be a sufficient biomarker for predicting cardiovascular diseases [24], [25] and diabetic retinopathy [26], as well as a prognostic indicator for evaluating the effect of drugs on the microcirculation [27], [28]. Besides, some diseases and stimuli can cause similar changes in both skin and brain vessels [29]. Our recent work suggests that skin vascular blood oxygen response to the vasomotor test has a good potential to serve as an assessment

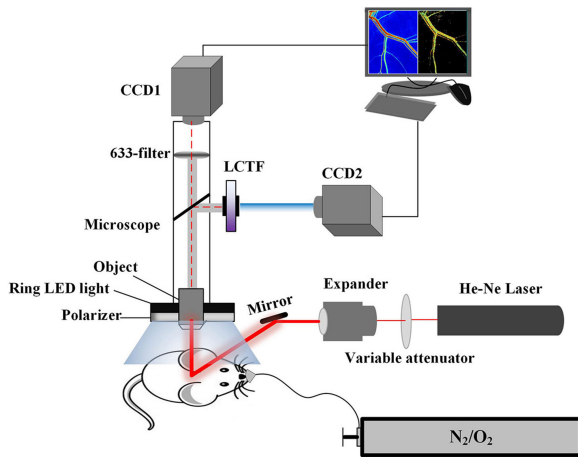


Fig. 1. Schematic of the imaging system.

indicator to predict the cerebrovascular dysfunction caused by type 1 diabetes [30]. As an easily accessible vascular bed, the peripheral skin will be a fine detection target for early warning to some brain diseases. At present, researches about the hemodynamic changes induced by hypoxia only focus on brain or skin separately, neglecting to establish their relations [8], [9]. Thus, the completion of comparative study between brain and skin microvascular functional changes induced by hypoxia can both reveal their relations and differences, and further illustrate whether skin vascular functional changes could be a potential indicator in diagnosing cerebrovascular dysfunction.

In this work, with the help of *in vivo* skull and skin optical clearing techniques, the dual-mode imaging system of HSI and LSCI was employed to simultaneously monitor the changes in blood flow and blood oxygen of cerebral and cutaneous microvessels with hypoxic stimulus. In addition, the rates of relative changes in blood oxygen and blood flow velocity for cerebral and cutaneous arteriovenous vessels were quantitatively analyzed during hypoxic challenge and recovery.

II. MATERIALS AND METHODS

A. Monitoring Hemodynamic Changes in Vascular Blood Flow and Blood Oxygen

Fig. 1 shows the schematic of imaging system. In order to simultaneously monitor vascular blood flow and blood oxygen, we combined the LSCI and HSI. This system mainly consists of two charge coupled device (CCD) cameras (Pixelfly USB, PCO Company, Germany), a liquid crystal tunable filter (LCTF, CRi Varispec VIS, Perkin Elmer, USA), a stereo microscopy (SZ61TR, Olympus, Japan), a ring-like LED light with a polarizer, a filter (633 ± 5 nm) and a He-Ne laser beam ($\lambda = 632.8$ nm, 3 mW) expanded by a collimating lens used to illuminate the areas of interest. The bandwidth of LCTF is 7 nm. A certified reflectance standard (SRS-99-020, Labsphere, USA) was used to acquire the standard hyperspectral images. All the hyperspectral images were acquired from 500 nm to 620 nm with a step size of 10 nm.

We used the algorithm developed previously to obtain blood oxygen saturation (SO_2) based on the hyperspectral dataset acquired by CCD2 [17], by which the arteries and veins can be well distinguished. The corresponding vascular blood flow can be obtained based on the recorded raw speckle images (The data was acquired by CCD1) by using laser speckle temporal contrast analysis method [31]. At 540 nm, both arteries and veins can be clearly observed due to the strong absorption of oxy-hemoglobin and deoxyhemoglobin. But at the wavelength of 620 nm, the absorption of deoxyhemoglobin is much higher than that of oxy-hemoglobin, thus, only the vein with rich deoxyhemoglobin can be clearly identified in the image. By this means, the artery and vein can be well distinguished.

B. Animal Preparation

Experimental procedures and animal care were approved by the Experimental Animal Management Ordinance of Hubei Province, P. R. China. Male BALB/c mice (25 ± 2 g, 8 weeks old, $n = 10$) were supplied by Wuhan University Center for Animal Experiment (Wuhan, P. R. China) and fed under specific pathogen free (SPF) level of feeding condition. All experimental procedures were performed according to animal experiment guidelines of the Experimental Animal Management Ordinance of Hubei Province, P. R. China, and the guidelines from the Huazhong University of Science and Technology, which have been approved by the Institutional Animal Ethics Committee of Huazhong University of Science and Technology.

C. *In Vivo* Skull and Skin Optical Clearing Techniques

Here, we used the newly-developed *in vivo* skin optical clearing technique to establish the optical clearing skin window for monitoring the subcutaneous vessels with the high resolution. After the hair removal, skin optical clearing agent (skin-OCA) was topically applied on the region of interest on dorsal skin, which was mixed with polyethylene glycol, thiazone and sucrose (67.1% wt/wt) at a volume ratio of 9:1:10 according to our previous work [32]. 15 min later, the treated skin became optically transparent, and cutaneous vessels can be well observed in this work [32].

The recently-developed *in vivo* skull optical clearing technique allow us to noninvasively monitor the cortical vessels through the intact skull. Firstly, the head hair was removed and an incision was made on the skin, then we used the skull optical clearing agent (skull-OCA) to establish the optical clearing skull window. About 15 min later, the exposed skull became optically transparent. The details about the preparation of *in vivo* skull optical clearing agent can refer to our recent work [22].

D. Hypoxia Experiment

At the normal state, mouse breathed the mixed gas (20% oxygen/78.5% nitrogen) under 1.5% isoflurane prior to the start of hypoxia phase. Then, the mouse was switched from the oxygen enriched air to another mixed gas (10% oxygen/ 88.5% nitrogen) with 1.5% isoflurane, and the hypoxia stimulus was maintained for 3 mins followed by a 4 min recovery period in

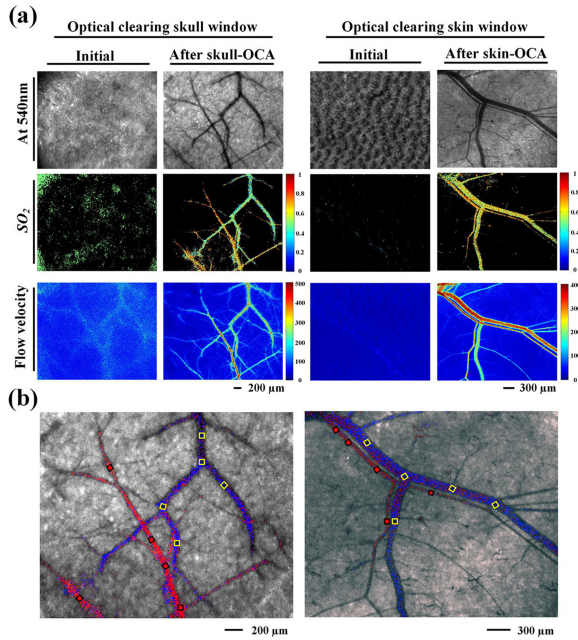


Fig. 2. Cortical/subcutaneous microvessels images before and after optical clearing treatment. (a) Left: the image at 540 nm, SO_2 and blood velocity maps of cortical vessels before and after skull optical clearing treatment. Right: the white-light, SO_2 and blood velocity maps of subcutaneous vessels before and after skin optical clearing treatment. (b) The maps of cerebral and cutaneous vessels extraction, respectively. The vessels colored by red are arteries, and the blue ones represent veins. The black and yellow rectangular regions were selected for SO_2 and blood flow velocity analysis.

which the oxygen and nitrogen were switched back to the 20% oxygen/78.5% nitrogen. And the data were recorded for 3 min at 10 seconds interval before hypoxia.

III. RESULTS

A. Visualization of Cortical and Cutaneous Microvessels By Using *In Vivo* Optical Clearing Techniques

Here, the dual-mode system of HSI and LSCI was employed to simultaneously monitor the SO_2 and blood flow velocity changes in cortical and cutaneous microvessels. Fig. 2 shows the cortical and subcutaneous microvessels images before and after skull and skin optical clearing. Due to the high scattering properties of the intact skull and skin, it is difficult to distinguish cortical and cutaneous microvessels through skull and skin at 540 nm (Fig. 2(a)). Whereas, the cortical and cutaneous microvessels were clearly observed after the optical clearing skull and skin windows establishment, and the imaging contrast was greatly improved. Thus, the cortical and cutaneous microvascular SO_2 and blood flow velocity maps could be obtained with the high resolution (Fig. 2(a)).

Moreover, based on the differences between the extinction coefficients of oxy- and deoxy-hemoglobin, the arteries and veins were extracted and colored by red and blue, respectively (Fig. 2(b)). The result shows that *in vivo* optical clearing techniques can improve the imaging quality dramatically, which permits to simultaneously monitor the cortical and cutaneous

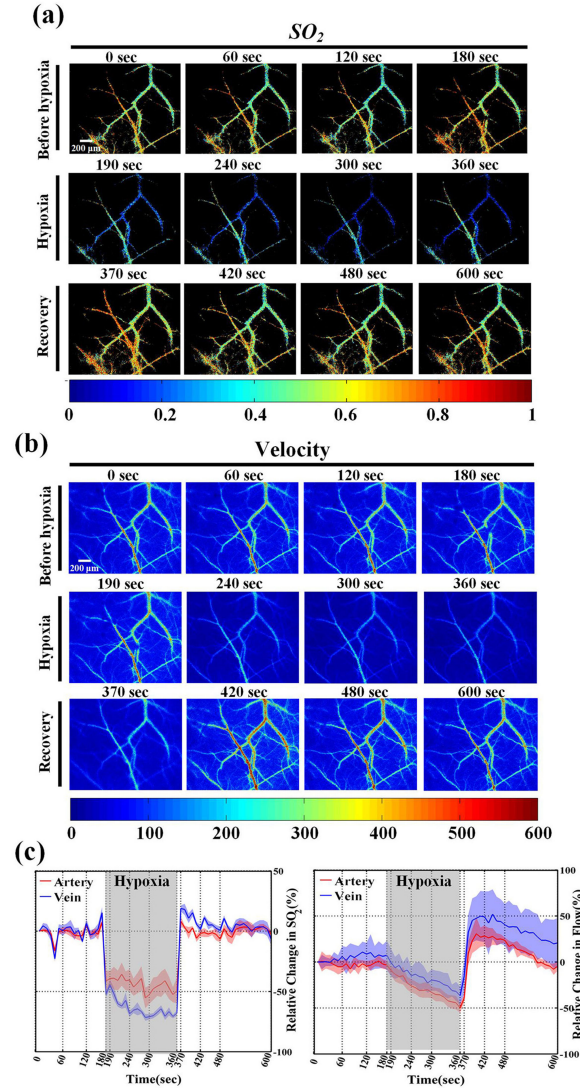


Fig. 3. Monitoring SO_2 and blood flow velocity changes in cerebral microvessels. (a) The pseudo-colored images show the spatiotemporal changes of SO_2 maps in the cerebral microvessels at initial, hypoxia and recovery phases through optical clearing skull window. (b) The pseudo-colored images show the spatiotemporal changes of blood flow velocity maps in the cerebral microvessels at initial, hypoxia and recovery phases. (c) The statistic graphs show relative changes in SO_2 and blood flow velocity of the arteries and veins at different states. The gray shade area indicates the hypoxic stimulus phase. And the curves and the width of shadows are mean and standard deviation, respectively. (Scale bar: 200 μm).

microvascular SO_2 and blood flow velocity changes by HSI and LSCI with high spatial resolutions.

B. Monitoring Cortical Microvascular SO_2 and Blood Flow Velocity Changes to Hypoxia

Further, we simultaneously monitored the cortical microvascular SO_2 and blood flow responses to the hypoxic stimulus. Fig. 3 shows the dynamic changes in cortical microvascular SO_2 and blood flow velocity at initial, hypoxia and recovery phases. When the hypoxic stimulus was implemented, both SO_2 and blood flow velocity of cortical microvessels decreased as shown in Fig. 3(a) and (b). And after hypoxia stimulus, cortical

microvascular SO_2 and blood flow velocity could be almost back to the original level.

In addition, we quantitatively analyzed the arteriovenous vascular relative changes in both SO_2 and blood flow velocity via the black and yellow rectangular regions as indicated in Fig. 2(b). Results showed that the SO_2 had a sharp decline when hypoxia stimulus occurred. Compared with the initial, the arteries decreased by $\sim 40\text{--}50\%$, and the veins reduced by $\sim 50\text{--}70\%$ at the duration of hypoxia. For blood flow velocity, during the hypoxia course, it steadily decreased, and the falling range was slower than that of SO_2 . During the recovery, the SO_2 quickly recovered and was nearly comparable with that in initial. But the blood flow velocity increased to a much higher level and then gradually declined (Fig. 3(c)). The result indicated that hypoxic stimulus not only caused changes in the microvascular blood oxygen but also in the blood flow, nevertheless, there are some differences in their trends.

C. Monitoring Cutaneous Microvascular SO_2 and Blood Flow Velocity Changes to Hypoxia

Additionally, the changes of cutaneous microvascular SO_2 and blood flow induced by hypoxia were also monitored with the help of *in vivo* skin clearing technique as shown in Fig. 4. Compared with the response of cerebral microvessels, similarly, the SO_2 and blood flow velocity of arteries and veins in cutaneous microvessels obviously decreased during hypoxic phase. And during recovery, the SO_2 and blood flow velocity of both arteries and veins increased (Fig. 4(a) and (b)). Further, we quantitatively analyzed the arteriovenous vascular relative changes of SO_2 and blood flow velocity via the selected regions as indicated in Fig. 2(b). Results showed that the SO_2 of the arteries and veins quickly decreased by $\sim 40\text{--}50\%$ at the duration of hypoxia compared with the initial. And during the recovery, the arteriovenous vascular SO_2 steadily became back to the normal state. As for blood flow velocity, hypoxia caused a small reduction. The blood flow velocity decreased by $\sim 13\%$ in veins and $\sim 20\%$ in arteries at the end of hypoxia, and about 1 min after recovery, the blood flow was nearly back to the initial (Fig. 4(c)). The results showed that the skin microvascular blood oxygen response was similar with the cortical microvessels under the hypoxic stimulus, but there were some differences between skin and brain microvessels in the trend of blood flow.

D. The Comparative Analysis for Cerebral and Cutaneous Vascular Responses to Hypoxia

Meanwhile, we quantitatively compared the cortical and cutaneous vascular responses to the hypoxia. The hypoxic response rate was defined as the relative change rate between the moment of starting hypoxia and 20 sec after starting hypoxia, and the recovery rate was defined as the relative change rate between the moment of starting recovery and 20 sec after starting recovery. Fig. 5 shows that the hypoxic response rate and recovery rate of blood flow velocity in cerebral vessels are significantly higher than cutaneous vessels.

And as for hypoxic response rate of SO_2 in cerebral and cutaneous vessels, there was no significant difference for arteries

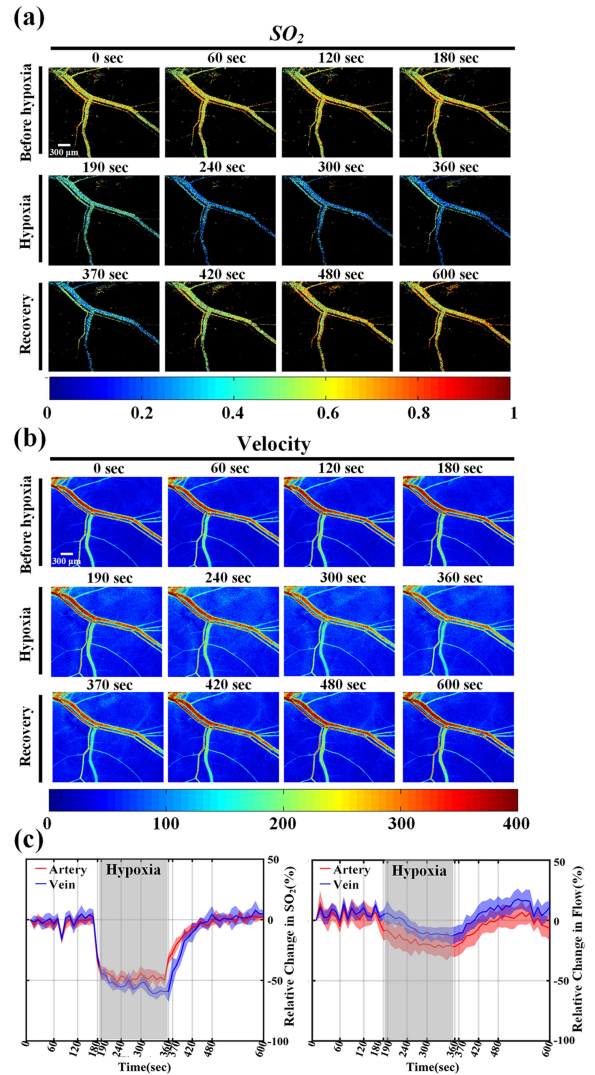


Fig. 4. Monitoring SO_2 and blood flow velocity changes in cutaneous microvessels. (a) The pseudo-colored images show the spatiotemporal changes of SO_2 maps in the cutaneous microvessels at initial, hypoxia and recovery phases through optical clearing skin window. (b) The pseudo-colored images show the spatiotemporal changes of blood flow velocity maps in the cutaneous microvessels at initial, hypoxia and recovery phases. (c) The statistic graphs show relative changes in SO_2 and blood flow velocity of the arteries and veins at different states. The gray shade area indicates the hypoxic stimulus phase. And the curves and the width of shadows are mean and standard deviation, respectively. (Scale bar: $300\ \mu\text{m}$).

but small significant difference for veins, and the recovery rate of SO_2 in cerebral was significantly higher than cutaneous vessels. These results indicated that cerebral vascular response was more sensitive than peripheral cutaneous vascular response to hypoxia, and the small decline of blood flow accompanied sharp decrease in SO_2 during hypoxia, but SO_2 did not continuously reduce but keep relatively stable.

IV. DISCUSSION

At present, *in vitro* tissue optical clearing technique plays an important role in 3D visualization of tissues, which can significantly enhance the imaging depth and resolution, allowing to acquire complete structural information of tissue blocks [33],

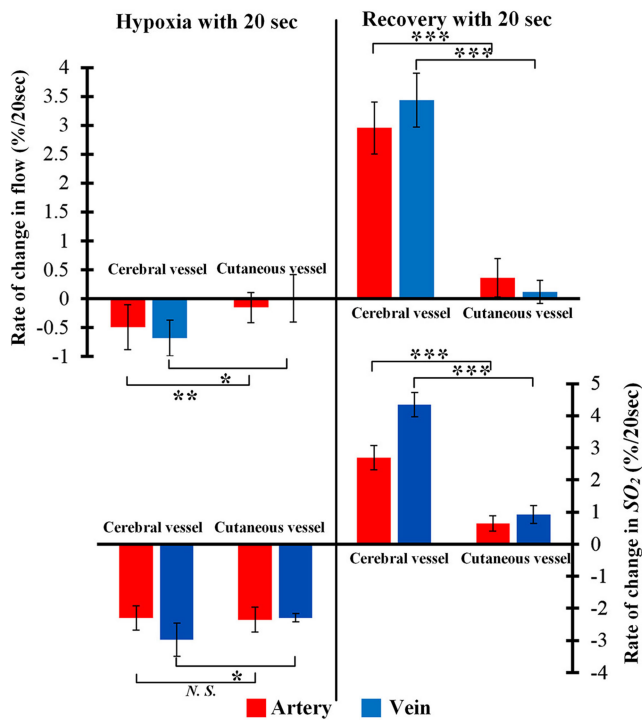


Fig. 5. The hypoxia rate and recovery rate of SO_2 and blood flow velocity in cerebral and cutaneous microvessels to hypoxia stimulus. The error bars indicate standard errors (S.E.). Data are shown as mean \pm S.E., $n = 5$. * <0.05 , ** <0.01 , *** <0.001 , N.S. no significant difference.

[34]. However, for *in vivo* optical imaging, the turbid property of tissue, e.g., skull and skin, still severely limits the imaging performances. Therefore, various optical imaging windows based on the surgical operations have been developed, including many types of skin window models [9], [35] and cranial window models [36], [37]. Nevertheless, the surgical operation will inevitably cause a series of inflammatory reactions, which may affect the structure and function of vessels and cells. Here, the skin-OCA and skull-OCA were applied to dramatically improve the imaging qualities of HSI and LSCI, which have been verified to be safe, and they would not cause observable affects to the structure and function of cutaneous and cerebral vessels [38], [39]. By combining these two optical clearing windows with HSI&LSCI, we realized visualization of monitoring the changes in cortical and cutaneous arteriovenous blood oxygen and blood flow.

By now, many *in vivo* skin optical clearing methods have been developed and applied towards different skin sites, such as dorsal skin, ear skin and footpad skin [40]–[42]. In this study, the newly developed skin-OCA was employed, with the advantages of fast transparency and better effects. However, this method is more suitable for mice because their skin is much thinner than others, including pig, human, etc. Certainly, some other *in vivo* skull optical clearing methods also have been proposed, for instance, the skull-OCA consisted a mixture of liquid paraffin and Vaseline [43] as well as laurinol, weak alkaline substances, EDTA, dimethyl sulfoxide, sorbitol, and glucose [23], [44]. Although these methods have identified their effectiveness for improving imaging qualities, their repeatability and safety have

not been verified. The *in vivo* skull clearing methods applied in this work has been identified to be safe, moreover, it allows to repeatedly applied to trace the cerebrovascular changes at the same region for 6 months [22]. However, it is unable to establish a permanent window by using this skull-OCA once. In the future, we will further optimize this skull optical clearing method to overcome this problem.

In this work, the cerebral and cutaneous vascular hemodynamic responses induced by hypoxia were monitored and quantitatively analyzed. Our results showed that the trend of blood oxygen response to hypoxia was more similar than that of blood flow response. It indicated that the changes in cortical and cutaneous vascular blood oxygen response to hypoxia might be more consistent than the blood flow. Although the trend of SO_2 in cutaneous vessels was similar with that of cerebral vessels, for the blood flow, the hypoxia-induced descent rate of cutaneous vessels was much lower than that of cerebral microvessels (Fig. 5). Additionally, we noticed that with the recovery of the breathing oxygen concentration, the cerebral blood flow increased immediately (Fig. 5), and the SO_2 could recover to the normal state instantly for rapid relief from the symptoms of hypoxia [45]. For the cutaneous microvessels, the recovery rates of both SO_2 and blood flow were slower than those of cerebral microvessels, which might attribute to the oxygen supply priority for the brain [45], [46]. In our recent work, we monitored the dynamic changes in the functional responses of cerebral and cutaneous vessels with the development of diabetes, and found that the cutaneous microvascular blood oxygen response had the potential to be an early warning target for the cerebrovascular dysfunction [30]. Additionally, some researchers suggest that there could be a link between cutaneous or systemic manifestations of amyloid deposits in Alzheimer's disease [47]. In fact, the skin offers an ideal detective site for investigating the peripheral and systemic responses to stress [48], and a stress-associated 'brain-skin connection' has been proposed [49]. By using some common and cost-effective detection methods on the skin, we can infer the dynamic changes of the cortex in some cases, avoiding the high cost or invasiveness for brain detection. Thus, the connections between brain and skin in various diseases is necessary to be investigated.

In hypoxia studies, isoflurane is often used for anesthesia to avoid the influence of body movements on imaging [50]. Some researchers made the comparison of hemodynamic changes in response to hypoxia between awake and anesthetized rat [51], and found that isoflurane could attenuate autonomic responses to hypoxia. This may be because isoflurane is a vasodilator, or isoflurane could abolish autoregulation of cerebral blood flow [52]. In this work, referring to the previous anesthetic strategies, the same concentration of isoflurane was kept during the whole experimental process to ensure the mice maintained at a relatively stable anesthetic state [50], [51]. And before the hypoxia stimulus, the SO_2 and blood flow were monitored for 180 seconds that fluctuated slightly as shown in Fig. 3(c) and Fig. 4(c). In the future, we will further improve and optimize the experimental techniques to realize the hemodynamic monitoring on awake mice, by which we can obtain more accurate vascular response excluding the effect of anesthesia. Similar

with other study, the cerebral blood oxygen decreased during the hypoxia [53]. Besides, our results showed that the cortical arteriovenous blood flow also decreased after hypoxia, which was consistent with René Schiffner *et al.*'s findings [54]. Ashley D. Harris' research found that across the grey matter, cerebral blood flow increased by approximately 15% over the course of hypoxia [55]. But the latest study reported that the subcortical blood flow increased, whereas the cortical blood flow decreased in comparison to baseline values during hypoxia [54]. These findings suggest that there may be differences in cerebral blood flow response in different brain regions to hypoxia.

The cerebral blood flow can be adjusted by systematic autoregulation, which depends on the duration of hypoxia, species, tissue type, as well as level and type of anesthetic [51], [56]. Additionally, a previous study has shown the general mathematical model between changes in cerebrovascular blood flow and oxygen metabolism, in which the blood flow and oxygen consumption are tightly coupled in a non-linear fashion [57]. As for the skin, it has been verified that there exists a causal relationship between skin blood flow and blood oxygen saturation [58]. And F. Tayyari *et al.* found that there was a relationship between retinal blood flow and blood oxygen saturation, but the correlations of the blood flow and blood oxygen saturation between veins and arteries were different [59]. In this study, we monitored the changes of blood flow and blood oxygen in cerebral and cutaneous arteriovenous microvessels during hypoxia, respectively. Our results are consistent with these previous studies. Besides, it demonstrates that the coupling between blood flow and oxygen metabolism in different tissues and organs may be different.

V. CONCLUSION

In this work, *in vivo* skull and skin optical clearing techniques were used for visualization of the cortical and cutaneous microvessels. And we combined the HSI and LSCI imaging systems to simultaneously monitor the cortical and cutaneous arteriovenous blood oxygen and blood flow changes to the hypoxic stimulus with the high spatial-temporal resolutions. The results demonstrated that the cutaneous microvascular blood oxygen response was similar with that of cortical microvessels under the hypoxic stimulus, but the trends of blood flow for cortical and cutaneous microvessels were different. Additionally, the quantitative results suggested that the cerebrovascular response was more sensitive than peripheral skin response to the hypoxic stimulus and recovery. This work provides a feasible approach to *in vivo* monitor cerebral and cutaneous microvascular functional responses, contributing to revealing the relations between cerebrovascular and peripheral circulation.

ACKNOWLEDGMENT

The data were acquired in Prof. Dan Zhu's lab, Britton Chance Center for Biomedical Photonics, Wuhan National Laboratory for Optoelectronics in Huazhong University of Science and Technology. We thank the Optical Bioimaging Core Facility of WNLO-HUST for help with the imaging setup.

REFERENCES

- [1] R. E. Airley, J. E. Monaghan, and I. J. Stratford, "Hypoxia and disease: Opportunities for novel diagnostic and therapeutic prodrug strategies," *Pharmaceut. J.*, vol. 264, no. 7094, pp. 666–673, Apr. 2000.
- [2] M. Nishikawa, "Reactive oxygen species in tumor metastasis," *Cancer Lett.*, vol. 266, no. 1, pp. 53–59, Jul. 2008.
- [3] C. G. Ellis, J. E. Jagger, and M. D. Sharpe, "The microcirculation as a functional system," *Crit. Care*, vol. 9, no. 4, pp. 1–6, Aug. 2005.
- [4] J. W. Cannon, "Hemorrhagic shock," *New England J. Med.*, vol. 378, no. 4, pp. 370–379, Jan. 2018.
- [5] A. T. Mazzeo and D. Gupta, "Monitoring the injured brain," *J. Neurosurg. Sci.*, vol. 62, no. 5, pp. 549–562, Oct. 2018.
- [6] X. Wei *et al.*, "IFATS collection: The conditioned media of adipose stromal cells protect against hypoxia ischemia induced brain damage in neonatal rats," *Stem Cells*, vol. 27, no. 2, pp. 478–488, Feb. 2009.
- [7] M. Horiuchi J. Endo, and Y. Handakirihra, "Relationship between cerebral oxygenation and skin blood flow at the frontal lobe during progressive hypoxia: Impact of acute hypotension," *Adv. Exp. Med. Biol.*, vol. 1232, pp. 69–75, Jan. 2020.
- [8] T. Q. Duong, C. Iadecola, and S. G. Kim, "Effect of hyperoxia, hypercapnia, and hypoxia on cerebral interstitial oxygen tension and cerebral blood flow," *Magn. Reson. Med.*, vol. 45, pp. 61–70, Jan. 2001.
- [9] G. M. Palmer *et al.*, "In vivo optical molecular imaging and analysis in mice using dorsal window chamber models applied to hypoxia, vasculature and fluorescent reporters," *Nature Protoc.*, vol. 6, pp. 1355–1366, Sep. 2011.
- [10] R. Shi *et al.*, "In vivo imaging the motility of monocyte/macrophage during inflammation in diabetic mice," *J. Biophoton.*, vol. 11, no. 5, 2018, Art. no. e201700205.
- [11] Z. Wei, Y. Zhang, and J. Yang, "Optical clearing-aided photoacoustic microscopy with enhanced resolution and imaging depth," *Opt. Lett.*, vol. 38, no. 14, pp. 2592–2595, Jul. 2013.
- [12] Y. Liu, X. Yang, D. Zhu, R. Shi, and Q. Luo, "Optical clearing agents improve photoacoustic imaging in the optical diffusive regime," *Opt. Lett.*, vol. 38, no. 20, pp. 4236–4239, Oct. 2013.
- [13] L. Guo *et al.*, "Optical coherence tomography angiography offers comprehensive evaluation of skin optical clearing in vivo by quantifying optical properties and blood flow imaging simultaneously," *J. Biomed. Opt.*, vol. 21, no. 8, Aug. 2016, Art. no. 081202.
- [14] K. V. Larin *et al.*, "Optical clearing for OCT image enhancement and in-depth monitoring of molecular diffusion," *IEEE J. Sel. Topics. Quantum Electron.*, vol. 18, no. 3, pp. 1244–1259, May/Jun. 2012.
- [15] X. Wen, S. L. Jacques, V. V. Tuchin, and D. Zhu, "Enhanced optical clearing of skin in vivo and optical coherence tomography in-depth imaging," *J. Biomed. Opt.*, vol. 17, no. 6, Jun. 2012, Art. no. 066022.
- [16] R. Shi, M. Chen, V. V. Tuchin, and D. Zhu, "Accessing to arteriovenous blood flow dynamics response using combined laser speckle contrast imaging and skin optical clearing," *Biomed. Opt. Exp.*, vol. 6, no. 6, pp. 1977–1989, Jun. 2015.
- [17] W. Feng, R. Shi, C. Zhang, T. Yu, and D. Zhu, "Lookup-table-based inverse model for mapping oxygen concentration of cutaneous microvessels using hyperspectral imaging," *Opt. Exp.*, pp. 3481–3495, Feb. 2017.
- [18] J. Wang *et al.*, "Sugar-Induced skin optical clearing: From molecular dynamics simulation to experimental demonstration," *IEEE J. Sel. Topics Quantum Electron.*, vol. 20, no. 2, pp. 56–62, Mar./Apr. 2014.
- [19] J. Wang, Y. Zhang, P. Li, Q. Luo, and D. Zhu, "Review: Tissue optical clearing window for blood flow monitoring," *IEEE J. Sel. Topics Quantum Electron.*, vol. 20, no. 2, pp. 92–103, Mar./Apr. 2014.
- [20] Y. J. Zhao *et al.*, "Skull optical clearing window for in vivo imaging of the mouse cortex at synaptic resolution," *Light Sci. Appl.*, vol. 7, Feb. 2018, Art. no. 17153.
- [21] X. Yang *et al.*, "Skull optical clearing solution for enhancing ultrasonic and photoacoustic imaging," *IEEE Trans. Med. Imag.*, vol. 35, no. 8, pp. 1903–1906, Aug. 2016.
- [22] C. Zhang, W. Feng, Y. J. Zhao, T. T. Yu, and D. Zhu, "A large, switchable optical clearing skull window for cerebrovascular imaging," *Theranostics*, vol. 8, no. 10, pp. 2696–2708, Apr. 2018.
- [23] J. Wang, Y. Zhang, T. H. Xu, Q. M. Luo, and D. Zhu, "An innovative transparent cranial window based on skull optical clearing," *Laser Phys. Lett.*, vol. 9, no. 6, pp. 469–473, Mar. 2012.
- [24] M. Hellmann, M. Roustid, and J. L. Cracowski, "Skin microvascular endothelial function as a biomarker in cardiovascular diseases?," *Pharmacol. Rep.*, vol. 67, no. 4, pp. 803–810, Aug. 2015.

- [25] E. G. Souza, L. A. De, G. Huguenin, G. M. Oliveira, and E. Tibiriçá, "Impairment of systemic microvascular endothelial and smooth muscle function in individuals with early-onset coronary artery disease: Studies with laser speckle contrast imaging," *Coronary Artery Dis.*, vol. 25, no. 1, pp. 23–28, Jan. 2014.
- [26] T. T. Nguyen *et al.*, "Diabetic retinopathy is related to both endothelium-dependent and -Independent responses of skin microvascular flow," *Diabetes Care*, vol. 34, no. 6, pp. 1389–1393, Jun. 2011.
- [27] M. Roustit and J. L. Cracowski, "Assessment of endothelial and neurovascular function in human skin microcirculation," *Trends Pharmacol. Sci.*, vol. 34, no. 7, pp. 373–384, Jul. 2013.
- [28] J. L. Cracowski, F. Gaillard-Bigot, C. Cracowski, M. Roustit, and C. Millet, "Skin microdialysis coupled with laser speckle contrast imaging to assess microvascular reactivity," *Microvasc. Res.*, vol. 82, no. 3, pp. 333–338, Jul. 2011.
- [29] Y. Shi and P. M. Vanhoutte, "Macro- and microvascular endothelial dysfunction in diabetes," *J. Diabetes*, vol. 9, no. 5, pp. 434–449, May 2017.
- [30] W. Feng *et al.*, "Comparison of cerebral and cutaneous microvascular dysfunction with the development of type 1 diabetes," *Theranostics*, vol. 9, no. 20, pp. 5854–5868, Aug. 2019.
- [31] J. Senarathna, A. Rege, N. Li, and N. V. Thakor, "Laser speckle contrast imaging: Theory, instrumentation and applications," *IEEE Rev. Biomed. Eng.*, vol. 6, pp. 99–110, Jan. 2013.
- [32] R. Shi *et al.*, "A useful way to develop effective *in vivo* skin optical clearing agents," *J. Biophoton.*, vol. 10, no. 6/7, pp. 887–895, Dec. 2016.
- [33] T. Yu, Y. Qi, H. Gong, Q. Luo, and D. Zhu, "Optical clearing for multi-scale biological tissues," *J. Biophoton.*, vol. 11, no. 2, Oct. 2017, Art. no. e201700187.
- [34] E. C. Costa, A. F. Moreira, D. De Melodiogo, and I. J. Correia, "ClearT immersion optical clearing method for intact 3D spheroids imaging through confocal laser scanning microscopy," *Opt. Laser Technol.*, vol. 106, pp. 94–99, Oct. 2018.
- [35] L. Ritsma *et al.*, "Surgical implantation of an abdominal imaging window for intravital microscopy," *Nature Protoc.*, vol. 8, no. 3, pp. 583–594, Mar. 2013.
- [36] A. Holtmaat *et al.*, "Long-term, high-resolution imaging in the mouse neocortex through a chronic cranial window," *Nature Protoc.*, vol. 4, no. 8, pp. 1128–1144, Jul. 2009.
- [37] D. Dorand, D. S. Barkauskas, T. A. Evans, A. Petrosiute, and A. Y. Huang, "Comparison of intravital thinned skull and cranial window approaches to study CNS immunobiology in the mouse cortex," *Intravital*, vol. 3, no. 2, May 2014, Art. no. e29728.
- [38] D. Zhu, K. V. Larin, Q. M. Luo, and V. V. Tuchin, "Recent progress in tissue optical clearing," *Laser Photon. Rev.*, vol. 7, no. 5, pp. 732–757, Sep. 2013.
- [39] D. Li, Z. Zheng, T. Yu, B. Tang, and D. Zhu, "Visible-near infrared-II skull optical clearing window for *in vivo* cortical vasculature imaging and targeted manipulation," *J. Biophoton.*, vol. 13, no. 10, Oct. 2020, Art. no. 202000142.
- [40] J. Wang, R. Shi, Y. Zhang, and D. Zhu, "Ear skin optical clearing for improving blood flow imaging," *Photon. Lasers Med.*, vol. 2, no. 1, pp. 37–44, Jan. 2013.
- [41] R. Shi, W. Feng, C. Zhang, Z. H. Zhang, and D. Zhu, "FSOCA-induced switchable footpad skin optical clearing window for blood flow and cell imaging *in vivo*," *J. Biophoton.*, vol. 10, no. 12, pp. 1647–1656, Dec. 2017.
- [42] D. Zhu, J. Wang, Z. Zhi, X. Wen, and Q. Luo, "Imaging dermal blood flow through the intact rat skin with an optical clearing method," *J. Biomed. Opt.*, vol. 15, no. 2, Jan. 2010, Art. no. 026088.
- [43] M. Tohmi, H. Kitaura, S. Komagata, M. Kudoh, and K. Shibuki, "Enduring critical period plasticity visualized by transcranial flavoprotein imaging in mouse primary visual cortex," *J. Neurosci.*, vol. 26, no. 45, pp. 11775–11785, Nov. 2006.
- [44] Y. Zhang, C. Zhang, X. Zhong, and D. Zhu, "Quantitative evaluation of SOCS-induced optical clearing efficiency of skull," *Quantitative Imag. Med. Surg.*, vol. 5, no. 1, pp. 136–142, Feb. 2015.
- [45] G. J. Bouma and J. P. Muizelaar, "Cerebral blood flow in severe clinical head injury," *New Horiz.*, vol. 3, no. 3, pp. 384–394, Aug. 1995.
- [46] M. K. Cho *et al.*, "Overexpression of KAI1 protein in diabetic skin tissues," *Arch. Plast. Surg.*, vol. 41, no. 3, pp. 248–252, May 2014.
- [47] G. Awal and S. Kaur, "Association of cutaneous amyloidosis with neurodegenerative amyloidosis: Correlation or coincidence?" *J. Clin. Aesthetic Dermatol.*, vol. 11, no. 4, pp. 24–27, Apr. 2018.
- [48] R. Paus, T. C. Theoharides, and P. C. Arck, "Neuroimmunoendocrine circuitry of the 'brain-skin connection,'" *Trends Immunol.*, vol. 27, no. 1, pp. 32–39, Jan. 2006.
- [49] S. Schreml, E. Kaiser, M. Landthaler, R. M. Szeimies, and P. Babilas, "Amyloid in skin and brain: What's the link?" *Exp. Dermatol.*, vol. 19, no. 11, pp. 953–957, Nov. 2010.
- [50] T. Wood *et al.*, "Monitoring of cerebral blood flow during hypoxia-ischemia and resuscitation in the neonatal rat using laser speckle imaging," *Physiol. Rep.*, vol. 4, no. 7, Apr. 2016, Art. no. e12749.
- [51] T. Q. Duong, "Cerebral blood flow and BOLD fMRI responses to hypoxia in awake and anesthetized rats," *Brain Res.*, vol. 1135, no. 1, pp. 186–194, Mar. 2007.
- [52] Z. Wang, B. Schuler, O. Vogel, M. Arras, and J. Vogel, "What is the optimal anesthetic protocol for measurements of cerebral autoregulation in spontaneously breathing mice?," *Exp. Brain Res.*, vol. 207, no. 3/4, pp. 249–258, Dec. 2010.
- [53] L. Borgström, H. Jóhannsson, and B. K. Siesjö, "The relationship between arterial PO₂ and cerebral blood flow in hypoxic hypoxia," *Acta Physiol. Scand.*, vol. 93, no. 3, pp. 423–432, Mar. 1975.
- [54] R. Schiffner *et al.*, "Altered cerebral blood flow and potential neuroprotective effect of human relaxin-2 (Serelaxin) during hypoxia or severe hypovolemia in a sheep model," *Int. J. Mol. Sci.*, vol. 21, no. 5, Feb. 2020, Art. no. 1632.
- [55] A. D. Harris *et al.*, "Cerebral blood flow response to acute hypoxic hypoxia," *NMR Biomed.*, vol. 26, no. 12, pp. 1844–1852, Dec. 2013.
- [56] B. K. Siesjö, *Brain energy metabolism*. New York, NY, USA: Wiley, 1978.
- [57] R. B. Buxton and L. R. Frank, "A model for the coupling between cerebral blood flow and oxygen metabolism during neural stimulation," *J. Cereb. Blood Flow Metab.*, vol. 17, no. 1, pp. 64–72, Jan. 1997.
- [58] A. Bernjak, A. Stefanovska, P. V. E. McClintock, P. J. Owenlynn, and P. B. M. Clarkson, "Coherence between fluctuations in blood flow and oxygen saturation," *Fluctuation Noise Lett.*, vol. 11, no. 1, Dec. 2012, Art. no. 1240013.
- [59] F. Tayyari *et al.*, "Retinal blood flow and retinal blood oxygen saturation in mild to moderate diabetic retinopathy," *Invest. Ophthalmol. Vis. Sci.*, vol. 56, no. 11, pp. 6796–6800, Oct. 2015.

Wei Feng received the B.S. degree in bioinformatics and the Ph.D. degree in biomedical engineering from the Huazhong University of Science and Technology, Wuhan, China, in 2014 and June 2019, respectively. He is currently an Assistant Research Fellow with the Central People's Hospital of Zhanjiang, Zhanjiang, China. His research interests include biomedical photonics and *in vivo* tissue optical clearing.

Chao Zhang received the B.S. and Ph.D. degrees in biomedical engineering from the Huazhong University of Science and Technology, Wuhan, China, in 2014 and June 2019, respectively. She is currently an Assistant Research Fellow with the Central People's Hospital of Zhanjiang, Zhanjiang, China. Her research interests include develop multimode optical imaging methods to trace dynamic changes in blood flow and blood oxygen based on *in vivo* skin/skull optical clearing techniques.

Dan Zhu is currently a Distinguished Professor with the Huazhong University of Science and Technology, Wuhan, China and the Vice Director with Wuhan National Optoelectronics Laboratory, Wuhan, China. She has authored more than 150 papers. Her research interests include *in vivo* and *in vitro* tissue optical clearing methods for different usage, tissue optical imaging theory, methods, and applications. She was an Editorial Member or a Guest Editor of the *Scientific Reports*, the *Biomedical Optics Express*, the *Biomedical Optical*, the *Innovative Optical Health Sciences*, and the *Frontiers of Optoelectronics*. She is also a Fellow of SPIE and the Secretary General and Vice President with the Biomedical Photonics Committee of Chinese Optical Society.